

<https://doi.org/10.1038/s43247-026-03283-8>

Beavers can convert stream corridors to persistent carbon sinks

Check for updates

Lukas Hallberg¹✉, Annegret Larsen², Natalie Ceperley³, Raphael d'Epagnier³, Tom F. Brouwers², Bettina Schaepli³, Sarah Thurnheer⁴, Josep Barba⁵, Christof Angst⁶, Matthew Dennis⁷ & Joshua R. Larsen^{1,8}

Recent reintroductions of the Eurasian beaver (*Castor fiber*) across Europe represents an ecological shift with potential implications for carbon cycling in stream corridors. However, the capacity of beaver impacts to influence short- and long-term carbon fluxes, and the mechanisms that govern these changes, remains poorly understood. We present a comprehensive carbon budget of a beaver-influenced stream corridor, covering all major aqueous and atmospheric exchanges, as well as biomass and sedimentary carbon storages, from a beaver wetland in Switzerland. By integrating carbon flux measurements with hydrology and bathymetry, we identify dominant pathways and dynamics in gaseous carbon emissions. Annually, the beaver wetland was a net carbon sink ($98.3 \pm 34.4 \text{ t yr}^{-1}$), driven by subsurface removal of dissolved inorganic carbon. Carbon dioxide emissions were the dominant source of carbon loss, seasonally shifting the system to a net carbon source during summer water recession. Projecting the long-term sediment and deadwood storage following wetland infilling, our upper estimate of sequestered carbon was 1194 t ($10.1 \text{ t ha}^{-1} \text{ yr}^{-1}$), nearly an order of magnitude greater than without beaver modification. Our findings demonstrate that beaver-induced hydrological change is fundamentally reshaping carbon cycling and reinforces the relevance of headwater catchments in climate change mitigation strategies.

Stream corridors are central to the global carbon (C) cycle, mediating the transformation and transport of terrestrial C to the oceans and atmosphere^{1,2}. Headwater streams, though covering a small fraction of total river area, process disproportionate amounts of C via retention or export of dissolved and particulate forms^{3,4} and account for ~50% of global riverine gaseous C emissions⁵. However, current estimates largely overlook the transformative role of beavers, ecosystem engineers that through rapid expansion across Europe (*Castor fiber*, Fig. 1a) and North America (*Castor canadensis*) might affect the regional C cycle. By constructing dams, beavers have the potential to reshape headwater ecosystems, creating ponds and wetlands that fundamentally alter the aquatic-terrestrial interface and shift systems from purely lotic to alternate lentic and lotic conditions.

Beaver-modified stream corridors are ecosystem hotspots of biogeochemical activity⁶, with enhanced water residence time, sedimentation, and light availability promoting organic C burial, aquatic productivity,

greenhouse gas (GHG) emissions, and aquatic-terrestrial exchange⁷⁻⁹. Yet, the net effect of beaver activity on complete stream corridor C budgets remains unclear, particularly regarding the contribution and fate of dissolved inorganic carbon (DIC), which is often the dominant form of fluvial C¹⁰ but largely excluded from existing assessments. Therefore, the capacity for beaver wetlands to act as persistent C sinks or transient sources remains poorly constrained, as they uniquely transform both the aquatic and terrestrial domains of stream corridors.

Here, we present a comprehensive, annual C budget of a temperate beaver-influenced stream corridor, incorporating all major gaseous, dissolved, and particulate fluxes, alongside biomass, sediment storage, and the full reach-scale water balance. By combining the annual budget with estimated C sequestration rates integrated over 13 years, we assess whether beaver impacts can promote net C retention at seasonal to decadal scales and explore the long-term stability of stored C through extrapolations of sediment composition and burial. Our results reveal that beaver-mediated

¹School of Geography, Earth and Environmental Sciences, University of Birmingham, Birmingham, UK. ²Department of Soil Geography and Landscape, Wageningen University & Research, Wageningen, the Netherlands. ³Institute of Geography (GIUB) and Oeschger Centre for Climate Change Research (OCCR), University of Bern, Bern, Switzerland. ⁴Swiss Federal Institute for Forest, Snow and Landscape Research (WSL), Birmensdorf, Switzerland. ⁵CREAF, Bellaterra (Cerdanyola del Vallès), Catalonia, Spain. ⁶info fauna – Nationale Biberfachstelle, Neuchâtel, Switzerland. ⁷MCGIS, Department of Geography, University of Manchester, Manchester, UK. ⁸Birmingham Institute of Forest Research (BIFoR), University of Birmingham, Birmingham, UK. ✉e-mail: l.hallberg@bham.ac.uk

hydrological transformation enables substantial and sustained C accumulation, likely far greater than in their absence, driven primarily by subsurface DIC retention at the annual scale and by sedimentary storage and deadwood accumulation at the decadal scale. By upscaling these long-term storage estimates to beaver-compatible floodplains across Switzerland, we further provide the first national-scale assessment of beaver-mediated C storage potential.

Results and discussion

Beaver wetland water balance

A key control on aquatic mass fluxes and wetland extent is the reach-scale water balance. The distinct seasonal regime of the hydrology in the beaver wetland followed a cycle of peak water extent (January–April), followed by substantial subsurface losses (April–August), and then a gradual return to greater water extent (August–January; Fig. 1b). Along the 800 m beaver-

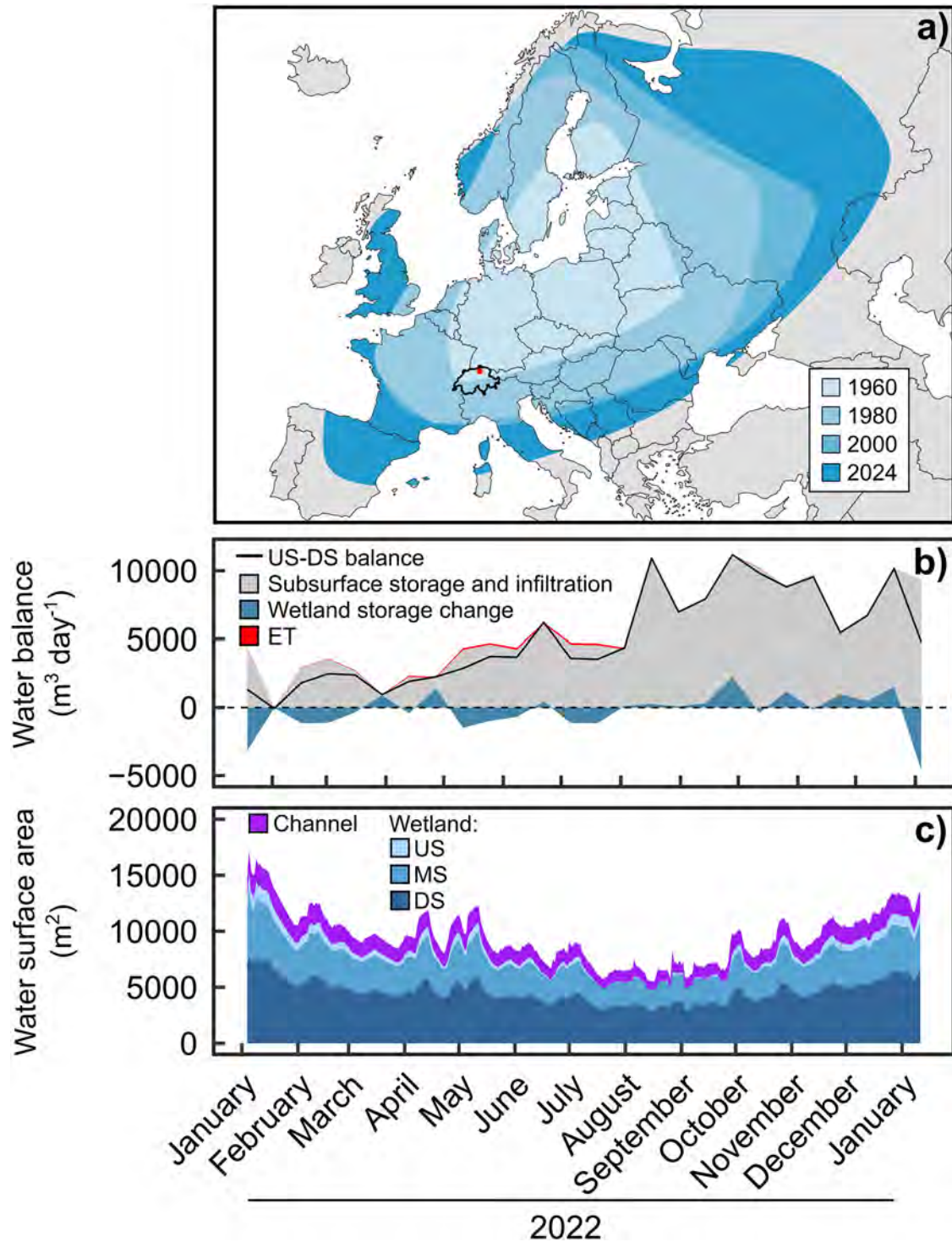


Fig. 1 | European beaver distribution and water balance in the studied beaver wetland. **a** Study site location in northern Switzerland (red point) and observed range of Eurasian beaver habitats in Europe from 1960 to 2024, based on data from the GBIF Backbone Taxonomy dataset (<https://doi.org/10.15468/39omei>, accessed via GBIF.org on 2024-12-11). **b** Fortnightly water balance between upstream (US)

and downstream (DS) locations. The water balance is partitioned into subsurface storage and infiltration, wetland surface storage change, and evapotranspiration (ET). Positive values denote water losses along the reach. **c** Daily water surface area in channel, upstream (US), midstream (MS), and downstream (DS) sections of the wetland.

impacted stream reach, we observed substantial and seasonally variable water losses between upstream and downstream, amounting to ~40% of annual inflowing discharge (Fig. 1b; Supplementary Fig. 1), which is consistent with annual water losses of 20–40% over similar distances in other beaver-modified systems^{11–13}. Yet, we note a greater uncertainty in water balance estimates during higher discharges ($> 0.5 \text{ m}^3 \text{ s}^{-1}$ at upstream); 11% and 14% of cumulative discharge in upstream and downstream rating curves, respectively, were extrapolated beyond the measured discharge range. Given the magnitude of the observed losses relative to the entire wetland surface area (3.6 ha), they cannot be explained by wetland storage and evapotranspiration alone and are instead primarily attributed to subsurface losses (Supplementary Text 1). The estimated average loss rate of 0.13 m day^{-1} is high for wetland systems, but physically plausible given the permeable gravel substrate¹⁴ and the elevated hydraulic gradients created by the impoundment¹⁵. Whilst this estimate is informative as a wetland average, in accordance with many dynamic wetland systems, the actual water losses are likely distributed across a wider range of lateral subsurface pathways that may extend well beyond the visible inundation boundary. These transient hydrological expansions activate lateral seepage and storage processes and could partially subsidise evapotranspiration in the surrounding forest.

Annual carbon budget of the beaver wetland

Hydrological transformation by beaver activity has profoundly restructured C cycling across the 800 m reach, resulting in a net annual C sink of $98.3 \pm 34.4 \text{ t C yr}^{-1}$, equivalent to 26% of total inputs (Table 1; Fig. 2a). In mass flux terms, this sink was dominated by the subsurface retention of DIC,

Table 1 | Annual budget of carbon fluxes in the beaver wetland

C species	C mass (t yr^{-1})
<i>Dissolved and gaseous C inputs</i>	
DIC	311.23 ± 28.24
DOC	23.65 ± 5.01
POC [*]	29.14 ± 8.25
CO ₂ -C _{atmosphere}	20.54 ± 0.19
Total inputs	384.56 ± 29.85
<i>Dissolved and gaseous C outputs</i>	
DIC	189.35 ± 13.96
DOC	15.46 ± 2.53
CO ₂ -C _{sediment}	76.40 ± 9.52
CO ₂ -C _{water}	3.50 ± 0.10
CO ₂ -C _{deadwood}	1.47 ± 0.27
CH ₄ -C _{total}	0.08 ± 0.14
Total outputs	286.26 ± 17.09
Mass balance	98.30 ± 34.39
<i>Cumulative C storages (2010–2022)</i>	
Sediment TOC	423.60 ± 117.90
Sediment TIC	161.73 ± 78.49
Green biomass TOC [†]	20.54 ± 0.20
Deadwood biomass TOC	500.40 ± 9.30
Total storage	1106.27 ± 141.94

^{*} Sediment C accumulation from deposition. Storage accumulation due to changes in sediment C content were not considered.

[†] Instantaneous annual rate, only reflecting green aboveground biomass and not its cumulative C input.

Carbon (C) inputs and outputs of dissolved, particulate, and gaseous C species, compared to annual C storage sediment and biomass, expressed as $\text{t C yr}^{-1} \pm$ one standard deviation. The mass balance is delimited to upstream and downstream monitoring locations of the beaver wetland. DIC dissolved inorganic carbon, DOC dissolved organic carbon, POC particulate organic carbon, CO₂-C carbon dioxide carbon, and CH₄-C methane carbon, TOC total organic carbon, and TIC total inorganic carbon.

accounting for more than half of all retained fluvial C, with additional contributions from particulate organic carbon (POC) burial (18%), and minor removal of dissolved organic carbon (DOC) (5%). While DOC accounted for a small fraction of total mass flux retention, actual concentrations consistently increased downstream, indicating net production within the wetland despite limited seasonal variation (Supplementary Fig. 2a). In contrast, carbon dioxide (CO₂) emissions from exposed sediments were the largest single C loss, though they did not offset the retained fluxes (Fig. 2a).

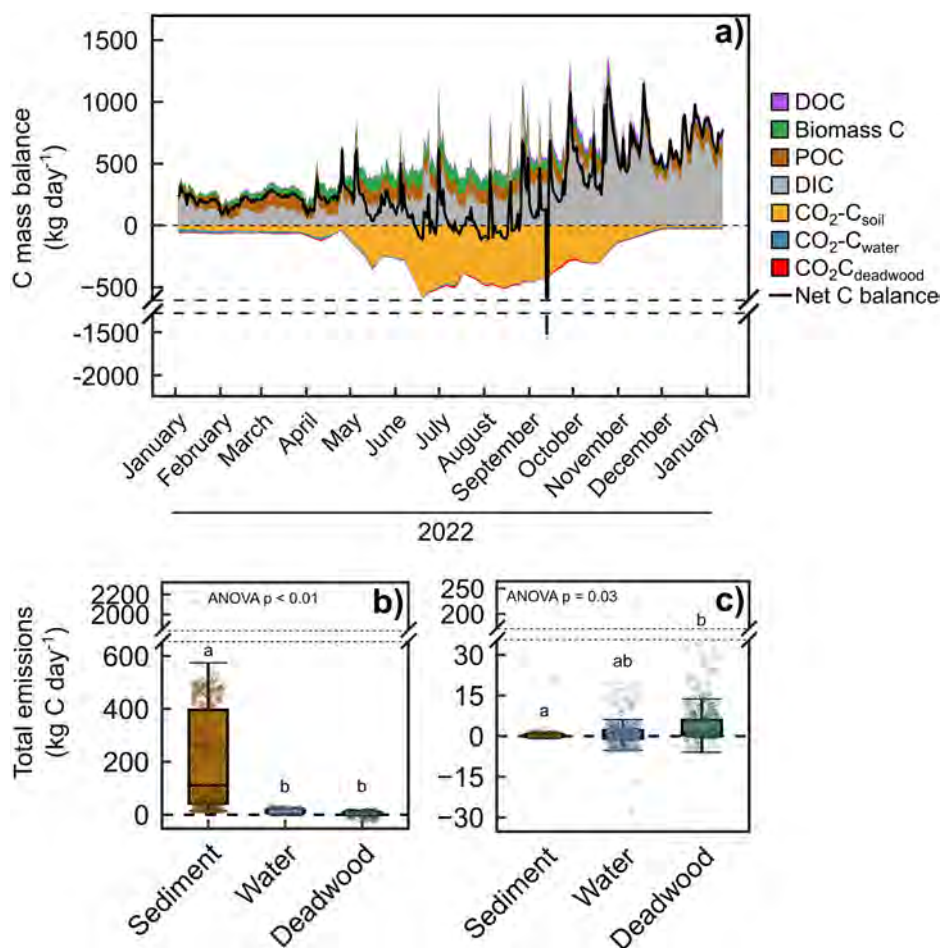
Carbon fluxes other than DOC exhibited strong spatial and seasonal variation, governed largely by dynamic shifts in surface water extent. During spring and early autumn (spring: March–May; summer: June–August; autumn: September–November; winter: December–February), greater inundation expanded the aquatic-terrestrial interface, enhancing subsurface DIC retention and diminishing the extent of aerobic CO₂ production. Although biological activity in the wetland seasonally altered DIC concentrations, there was overall a net balance between uptake/precipitation and dissolution/biogenic production of DIC (Supplementary Fig. 2b). As water levels receded in summer, increased exposure of wetland sediments enhanced CO₂ emissions, accounting for 93% of total gaseous C losses, while emissions from wetland water and deadwood remained low (Fig. 2b). Although DIC reductions scaled with CO₂ emissions from exposed sediments, CO₂ emissions peaked prior to the elevated DIC load reductions in autumn. Substantial outgassing of DIC as CO₂ was unlikely, as water CO₂ emissions were much lower than DIC losses, and the pH range in channel and wetland water (6.65–8.59) favoured the consistent dominance of bicarbonate. Thus, the large reach-scale reduction in DIC loads implies that C budgets from previous studies, which did not explicitly couple the C budget and water balance, may underestimate total C retention in active beaver stream corridors^{8,16}. Notably, excluding DIC reductions ($122 \pm 32 \text{ t C yr}^{-1}$) would shift the system from a net sink to a slight net C source. The DIC sink response was neither strongly impacted by discharge extrapolation beyond the measured range; when excluding DIC load changes for days with discharge estimates exceeding the measured range from salt additions (36 days), the resulting DIC reduction was 103 t C yr^{-1} . Reductions in POC were inferred from modelled sediment deposition rates (Supplementary Text 4) and represent a more uncertain component of the budget. However, the sediment trapping efficiency and reach geometry imply that downstream POC export is likely low relative to deposition.

The average CO₂-C fluxes from the beaver wetland did not differ from reference sites in the adjacent forest and upstream channel (t-test: $p = 0.30$). However, fluxes were redistributed across different ecosystem interfaces, wherein CO₂-C fluxes from exposed wetland sediments were higher than from forest soils, and from wetland water and deadwood were lower than the upstream channel and forest deadwood (Supplementary Fig. 3). This supports the interpretation that the wetland's net CO₂ flux was primarily driven by respiration in exposed sediments rather than by aquatic outgassing. Methane (CH₄) emissions were elevated over permanently inundated wetland zones, but CH₄-C emissions were negligible compared to the annual C balance ($< 0.1\%$; Fig. 2c). Further, CH₄ contributed only ~1% of the system's global warming potential, based on CO₂ equivalent calculations¹⁷, confirming that CO₂ was by far the dominant GHG. As a whole, the seasonally variable wetland area regulated both C retention and gaseous emissions by modulating hydrological connectivity, vegetation dynamics, and redox conditions.

Beaver-mediated sediment carbon burial and its implications for long-term sequestration

Sediment analyses showed that the beaver-created wetland substantially increased organic (1.5–8.1 times) and inorganic C contents (2.1–14.9 times), compared to adjacent forest soils or pre-beaver floodplain sediments, using a space-for-time approach (Fig. 3a). Both organic and inorganic C content in sediments were highest in permanently inundated areas, reflecting a compositional enrichment that likely results from reduced decomposition rates under anaerobic conditions and the accumulation of inorganic C

Fig. 2 | Temporally resolved C budget and GHG emissions from wetland interfaces. **a** Annual dynamics of daily C mass balance revealed seasonal shifts between sink-source behaviour in the beaver wetland, primarily driven by DIC retention and $\text{CO}_2\text{-C}$ emissions. The total C mass balance consists of changes in fluvial DOC, POC, and DIC loads between upstream and downstream locations; emissions of $\text{CO}_2\text{-C}$ from permanently and intermittently inundated sediments, downstream channel water surface, and deadwood in the studied beaver wetland; C in assimilated aquatic biomass. $\text{CH}_4\text{-C}$ emissions are not shown due to their negligible impact on the budget. Positive values denote C accumulation (C sink). Total emissions of **b** $\text{CO}_2\text{-C}$ and **c** $\text{CH}_4\text{-C}$ from exposed sediments (Sediment), wetland and downstream channel water (Water), and deadwood, across the entire beaver wetland. *P*-values of ANOVA tests and letters of Tukey's post-hoc tests are shown within panels.



through microbially mediated DIC precipitation. However, these sediments also showed a greater sensitivity to C mineralisation, reflected in the elevated C reactivity ratios (Fig. 3b). Despite this higher reactivity, both intermittently and permanently inundated wetland sediments exhibited relatively high proportions of stable C fractions (recalcitrant organic C and inorganic C content), indicating strong potential for long-term sequestration.

Deadwood storage, accounting for ~45% of the cumulative C storage (2010–2022), originated from a mixed riparian forest inundated following beaver dam construction. This represents a direct transformation of terrestrial biomass into longer lived aquatic and sedimentary C pools, and is likely to be a substantial though variable component of C storage in many beaver-impacted reaches. To contextualise these cumulative stores, we estimate an average annual sequestration rate of 46 t C yr^{-1} , based on 13 years of cumulative C storage, but excluding the deadwood inputs (Table 1). This is notably lower than the independently derived net C balance of $98.3 \pm 34.4 \text{ t C yr}^{-1}$ based on annual gaseous and dissolved fluxes, yet consistent with the expectation that only a fraction of the large annual sub-surface DIC losses is retained in the wetland as long-term storages through biogeochemical uptake and precipitation¹⁴. The fate of DIC entering groundwater remains largely unknown; infiltrated DIC may be conservatively stored in groundwater (decades to centuries), sequester as carbonates, but also propagate into C emissions through surface water^{18,19}.

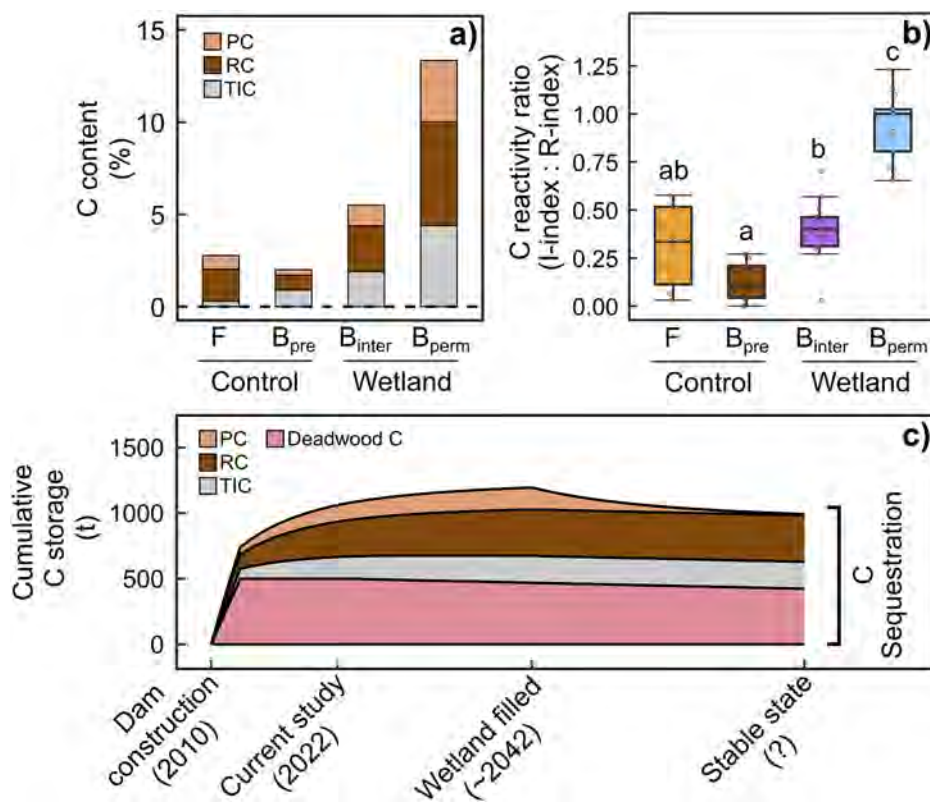
Projected forward, the combined storage in sediment and deadwood suggests the system could accumulate 1194 t C ($10.1 \text{ t C ha}^{-1} \text{ yr}^{-1}$) over its estimated active lifespan of ~33 years as actively maintained beaver habitat (Fig. 3c), representing an upper estimate after which the wetland is estimated to approach complete infilling and restrict beaver activity along the reach (Supplementary Text 4). This marks a key transition from annually

dynamic, water-coupled C fluxes to long-term burial and stabilisation, establishing the beaver-modified stream corridor as a persistent C sink. Over time, the proportion of labile C will decline through mineralisation, transitioning toward more recalcitrant and stable forms. This eventual compositional shift may ultimately lead to a stable state in long-term C storage, although the timing of this transition remains uncertain.

To benchmark the annual and long-term net C sink in the present beaver-modified system (Table 1), we constructed a counterfactual scenario representing the same stream corridor without beaver modification, combining empirical measurements from the present beaver-influenced system with physiologically and hydrologically constrained estimates of the same reach in its pre-beaver state (Fig. 4). In this scenario, flow would remain largely confined to the active channel, with minimal overbank inundation, negligible hydrological losses, and forested riparian soils (Supplementary Table 1; Supplementary Text 8). Under these conditions, analogous to other temperate headwaters over short distances (~800 m), C inputs would be limited to forest biomass growth (22.4 t C yr^{-1}), accumulation of coarse woody debris (3.2 t C yr^{-1}), and minor aquatic primary production (0.4 t C yr^{-1}). In contrast to the beaver system's annual net sink, the counterfactual scenario behaves only as a modest C sink ($0.5 \pm 1.9 \text{ t C yr}^{-1}$; Supplementary Table 1), in accordance with previous findings from stream-floodplain systems²⁰. When comparing the long-term C sequestration projections, it is evident that beaver-induced hydrological restructuring substantially alters the C storage potential in headwater stream corridors, enhancing C sequestration by approximately two orders of magnitude. By contrast, without such restructuring, these opportunities for seasonal C retention and long-term sequestration remain fundamentally limited.

When extrapolating the estimated long-term C burial rate (Fig. 3c) across all floodplain areas in Switzerland suitable for beaver recolonisation,

Fig. 3 | Sediment C quality and reactivity, and decadal projection of C stores. a Mean C content of pyrolysable organic C (PC), recalcitrant organic C (RC), and total inorganic C (TIC), in forest soils (F), floodplain sediments pre-beaver introduction (B_{pre}), intermittently inundated beaver wetland sediments (B_{inter}), and permanently inundated beaver wetland sediments (B_{perm}). **b** C reactivity ratio representing organic C stabilisation with lower values. I-index = preservation of PC and R-index = contribution of RC in sediments. Sediment and soil interfaces were compared using a one-way ANOVA with Tukey's post-hoc test, with letters indicating which interfaces are statistically different from one another ($p < 0.05$). **c** Projection of cumulative C mass storage of sediment and deadwood C fractions throughout beaver dam construction, complete sediment infilling of wetland, and stabilisation of C storage.



beaver-driven C burial could offset approximately 1.2–1.8% of the country's annual C emissions²¹, achieved solely through a nature-based solution requiring no active management or direct costs (Supplementary Text 9). By comparison, this represents only 2.4–3.6%²² of Switzerland's total forest area yet contributes an estimated 5–8%²² of the national forest C sink, underscoring the disproportionately high per-area C storage efficiency of beaver-modified floodplains. Here, long-term C burial rate was chosen as the appropriate comparison with national inventories as it represents the net sequestration over decadal to centennial scales, as opposed to the short-term annual cycling.

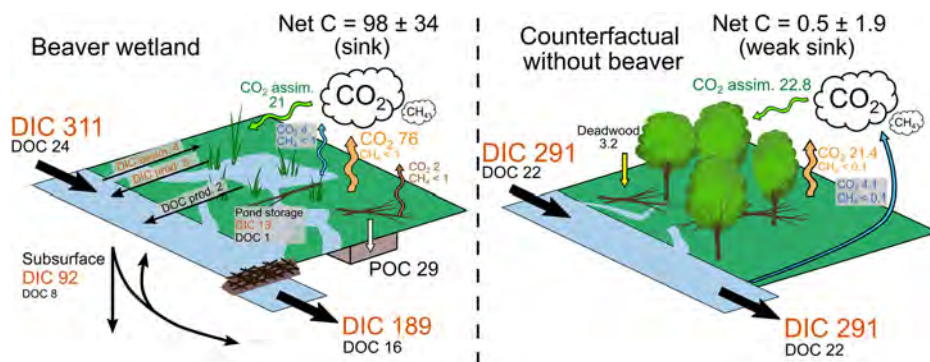
Regional implications of beaver impacts on the C cycle

The beaver-driven restructuring of subsurface hydrology and riparian connectivity accelerated C cycling across aquatic, terrestrial, and atmospheric interfaces, resulting in a C sink response rarely observed over stream reaches of similar length. This highlights a largely untapped potential to increase C retention in headwaters, where beavers transform stream corridors from passive systems into active control points for C cycling and burial. The beaver-impacted reach in this study is representative of semi-confined river valleys in a temperate continental climate, with the exception of its underlying Rhine gravels that likely enhance subsurface losses. Yet, our estimated stabilised sediment TOC storage (98 t ha⁻¹) was an order of magnitude lower than North American beaver systems (1150–1400 t ha⁻¹)⁹. Although this difference is likely attributed to lower upstream inputs of TOC, it may also partly reflect the higher sampling intensity and spatial resolution in our study, which captured a greater spatial heterogeneity and included more low-density zones, resulting in lower overall bulk density and therefore C content estimates. A similar pattern emerges for GHG fluxes, whereby our estimates (1.2 mg CO₂-C m⁻² day⁻¹; 0.09 mg CH₄-C m⁻² day⁻¹) were substantially lower than fluxes from North American beaver systems (4.9 mg CO₂-C m⁻² day⁻¹; 0.22 mg CH₄-C m⁻² day⁻¹)⁸. Prior GHG measurements have typically focused on boreal, peat-rich environments, where freeze-thaw cycles intensify organic matter mineralisation²³. Our study site's absence of these processes, along with non-peat substrates and presence of

alternative electron acceptors (N, Fe, and SO₄²⁻) that outcompete methanogenesis, likely explains these lower emissions and strongly suggests current global estimates of GHG fluxes from beaver wetlands may overestimate emissions by excluding more temperate and European regions⁸. Ebullitive CH₄ fluxes was not captured with our monitoring approach, a pathway that can account for up to 70% of total CH₄ emissions in wetlands^{24,25}. Yet, even if inferring a 70% fraction of ebullitive fluxes in the present study, total CH₄ emissions would still account for <0.5% of the total C mass balance. Thus, the lower organic C sediment and soil contents in the studied ecosystem and upstream contributing area may lower both magnitudes in TOC deposition and C emissions, compared to boreal systems. To refine regional and global assessments, along with future projections of beaver-mediated C cycling, greatly expanded monitoring of temperate European stream corridors is needed²⁶.

Despite uncertainties, the capacity for sediment burial to offset and exceed gaseous C emissions underscores the role of beavers as natural agents for buffering climate change. In comparative terms, our sediment TOC accumulation estimate is more than an order of magnitude higher than targeted C sequestration in agricultural soils from temperate regions^{27,28}. Nonetheless, these beaver-mediated C sinks remain spatially and temporally constrained, limited to headwater stream corridors susceptible to dam construction²⁹ and dependent on relatively short occupation timespans (1–20 years)⁷. Moreover, dam failure may result in rapid mobilisation and downstream export of deposited sediments, resulting in substantially lower sediment C storages upstream of the breached dam^{30,31}. Erosion of large sediment C stores following dam failure often results in local displacement sediments further downstream, maintaining C storages on a regional scale³⁰. Thus, our projected C storages in the studied beaver wetland are contingent on the system being maintained across 33 years. Yet, we chose to not include dam breaching as a scenario in our C budget estimates, given the stable conditions with intact dam integrity over 13 years, and unknown frequencies and magnitudes of dam failure. Although C deposits generated from beaver activity can persist over millennia³², their stability, especially of inorganic C, remains uncertain following infilling and meadow succession.

Fig. 4 | C pathways and mass balance for beaver wetland and counterfactual scenario. Black arrows show solute C pathways, white arrow shows POC deposition, and yellow arrow shows deadwood deposition. Gaseous C emissions are shown as blue (water), orange (sediment/soil), and photosynthetic assimilation is shown as green arrows. Values denote $\text{C yr}^{-1} \pm$ one standard deviation.



Moreover, behavioural unpredictability and limited control over site persistence pose challenges for beaver management, contrasting with the greater predictability of engineered stream solutions. The resurgence of beavers at a continental scale provides a timely motivation for understanding both active and legacy beaver impacts on stream corridors, which is essential to fully characterise their impact on aquatic-terrestrial C cycling.

Methods

Study area

The studied beaver wetland is located in a 2nd order stream, draining the lower part of a headwater catchment (28.7 km²) near Marthalen in Northern Switzerland (47.6° N, 8.6° E, 364 m a.s.l.), situated in the Rhine River basin (Supplementary Fig. 4a). The catchment's subsoil is dominated by thick layers of quaternary Rhine gravels and glacial till, in which shallow top soils have developed. The study area is an 800 m long, semi-confined stream-floodplain reach, with a perennial stream that was channelised and clay-lined in 1956. The beaver wetland has formed on the east side of the stream (Supplementary Fig. 4b) and is characterised by intermittent inundation in the up- and midstream sections, and permanent surface water cover in the downstream section. A small, artificial pond to trap sediments from an upstream quarry is located immediately upstream of the beaver wetland. Prior to the establishment of a beaver wetland in 2010, the study area was a forested floodplain, characterised by older, mixed stands of deciduous trees in the up- and midstream sections and younger plantations of coniferous trees in the downstream section. Since then, beaver activity has resulted in dieback of trees and opened the canopy in the active wetland area, promoting the proliferation of emergent macrophytes (e.g., *Phalaris arundinacea*, *Spartanium erectum*, and *Ceratophyllum demersum*) and micro algae.

Field data collection

The field data used in this study were collected between January 2022 and January 2023, with additional sediment depth measurements and sampling in March 2023 and April 2024. To quantify discharge (Q), we conducted fortnightly to monthly slug tracer tests³³ at US and DS locations in the study reach (Supplementary Fig. 4b). Sodium chloride (NaCl) was used as a tracer, injected at 75 m (US) and 150 m (DS) upstream of respective locations, determined from the recommended ≥ 25 times stream width (m). Break-through curves of NaCl tracer additions were measured as electrical conductivity (EC) at 15 s intervals using a Multi 3510 IDS probe (WTW, Germany). Water stage was monitored at US, midstream wetland, and DS using U20L-01 pressure sensors (Typical error: ± 0.01 m; HOBO, USA) deployed at channel and wetland beds, corrected for barometric air pressure, and logging at 15 min intervals. EC and water temperature were monitored at US and DS at 15 min intervals with U24-001 sensors (HOBO, USA).

Water grab samples were collected fortnightly at US and DS for analysis of DIC and DOC (filtered with 0.22 μm membrane), stored cool and dark (DOC), and delivered at the end of each sampling day to laboratories in the Swiss Federal Institute of Aquatic Science and Technology and the

University of Bern. DIC was derived from total alkalinity, which was determined by titration with standard acid using a Metrohm 809 Titrando to pH 8.3 and 4.5, providing carbonate and total alkalinity endpoints, respectively. Results were expressed in mmol L^{-1} and converted to C mass equivalents (mg C L^{-1}) by multiplying by the molar mass of C (12.011 g mol^{-1}). Given the observed pH range during our field sampling (6.65–8.59) and relatively moderate DOC concentrations (2.96–9.01 mg L^{-1}), the contribution of organic acids to total alkalinity can confidently be expected to be negligible. Concentrations of DOC were measured using a dry combustion method (DIN EN 1484, 1997).

The production rate of CO_2 and CH_4 was measured in the beaver wetland from exposed sediments, water surfaces (wetland and DS channel), and dead tree stems at fortnightly intervals between January and December 2022, using customised chambers connected to a calibrated LI-7810 gas analyser (LI-COR Biosciences, USA). Soil chambers (volume = 15.2 L, area = 4.3 dm^2) had static collars permanently installed for the year, made airtight with the chamber lid, water chambers (11.8 L, 7.5 dm^2) were closed and floating but not drifting, and tree chambers (0.5 L, 1.1 dm^2) were static and airtight. No chambers were ventilated since it was a closed measurement system. Each wetland interface was paired with additional CO_2 and CH_4 production rate measurements in reference sites adjacent to the wetland, including forest soil, US channel (100 m upstream of wetland) and US₂₅₀ channel (250 m upstream of wetland) and dead forest tree stems.

To quantify annual C input from vegetation in the wetland, present macrophyte species and micro algae were surveyed and sampled in the field. The spatial cover of vegetation was estimated using multispectral drone data, collected with RTK Phantom 4 and Mavic 2 Pro drones (DJI, China) between January and December 2022. The estimation of species-specific biomass is further described in Supplementary Text 2 and Supplementary Table 3.

Carbon content and quality were measured in wetland sediment and forest soil core samples collected in April 2024, from the beaver wetland ($n = 13$; depth = 10–90 cm) and adjacent forest ($n = 8$; depth = 10–45 cm). Sampling depths in the wetland reflects the entire post-beaver horizon (upper, loose and unconsolidated) and > 10 cm of pre-beaver horizon (lower, consolidated), where this was possible to sample. Forest cores were sampled to capture the O horizon and, if possible, the A horizon. Wetland sediments were separated into post-beaver and pre-beaver horizons, based on penetration resistance with a rod (Supplementary Text 4). Sediment TOC, TIC, and C quality fractions were determined from Rock-Eval pyrolysis, described in Supplementary Text 3. To derive total C storage and predict C sequestration potential in the wetland, sediment C content and quality were combined with modelled sediment volumes, deposited between 2010 and 2022 in the wetland, and respective bulk densities of samples. Modelled sediment volumes were based on point measurements of deposited sediment depths measured with a graduated rod and a soil corer in March 2023 and April 2024, respectively. Measured sediment depths were subsequently interpolated to sediment volume across the entire wetland (Supplementary Text 4).

Hydrological analyses

Stream Q ($\text{m}^3 \text{s}^{-1}$) during salt slug releases was estimated using the EC breakthrough curves of NaCl tracer additions as followingly:

$$Q = \frac{M}{\int (C - C_0) dt} \quad (1)$$

where M (g) is the mass of added NaCl, C is the observed NaCl concentration (g m^{-3}), C_0 is the background NaCl concentration (g m^{-3}). Since we could not establish a reliable relationship between EC and NaCl concentrations in field, we derived NaCl concentrations from the differences in ionic strength of tracer additions, compared to background stream water ionic strength, following the method of McCleskey et al.^{34,35}, described in Supplementary Text 5. Discharge estimates at upstream were further validated by Q at a station 1 km upstream (Supplementary Fig. 6a), monitored by Zurich Civil Engineering Office (511 Mederbach-Marthalen; <https://www.zh.ch/de/umwelt-tiere/wasser-gewaesser/messdaten/abfluss-wasserstand.html>).

Time series of continuous stream Q ($\text{m}^3 \text{s}^{-1}$) at US and DS were estimated by establishing power law stage- Q rating curves: $Q = a(h - h_0)^b$, where h (m) is the measured stage, h_0 (m) is the stage datum, and a and b are estimated coefficients. To ensure robust Q rating at US and DS locations, channel geometry and bank stability were assessed through repeated drone surveys and field inspections during the monitoring period, and no considerable morphological change was observed at either gauging location.

To determine the annual water balance within the study reach, Q losses between US and DS were partitioned into evapotranspiration, wetland storage change, and subsurface storage/infiltration. Evapotranspiration was estimated using the Priestley-Taylor equation³⁶. The calculations of evapotranspiration, water volumes and water balance are further described in Supplementary Text 6.

Modelling of dissolved carbon loads and gaseous carbon fluxes

To quantify changes in dissolved C mass in the beaver wetland, DIC and DOC loads at US and DS were modelled with a Weighted Regressions on Time, Discharge and Season (WRTDS) approach. Fortnightly DIC and DOC concentrations and continuous Q were used to model daily loads, using the R package *EGRET*³⁷. The goodness-of-fit of modelled loads are shown in Supplementary Table 5. Statistical confidence was estimated with *EGRETci*³⁸, using a bootstrap approach (n replicates = 400). To determine which processes that controlled changes in dissolved C loads, their turnover was partitioned into hydrological and biogeochemical pathways, as described in Supplementary Text 7.

Fluxes of $\text{CO}_2\text{-C}$ and $\text{CH}_4\text{-C}$ ($\text{g C m}^{-2} \text{day}^{-1}$) were quantified with the R package *gasfluxes*³⁹, using measured gas concentrations corrected for temperature, partial pressure, and chamber dimensions. Flux estimates resulted in 239 CO_2 samples and 242 CH_4 samples from the beaver wetland and 174 CO_2 samples and 174 CH_4 samples from the reference sites. To derive daily C flux estimates for subsequent spatial and annual scaling, we linearly interpolated fluxes between measured dates (R package *imputeTS*⁴⁰). This approach was chosen since no sediment temperature and water content data were available for predicting daily sediment C fluxes, and water C fluxes did not correlate with water temperature. Daily C fluxes were then scaled to total emissions by multiplying the daily area of each interface. Here, we used the estimated water surface areas (Supplementary Text 6; Supplementary Fig. 7) and deadwood area (Supplementary Text 2). Exposed area was determined as the difference between total surface area and water surface area. When multiplying sediment C fluxes with exposed surface areas, we did not account for antecedent conditions and the effect of higher moisture content on CO_2 fluxes in recently inundated sediments. However, when testing the effect of air temperature and exposed surface area (proxies for moisture condition) on measured sediment CO_2 fluxes with multiple linear regression, the exposed surface area did not explain the variation in CO_2 fluxes

(Supplementary Table 6). Spatial differences in C emissions and fluxes between wetland locations and forest reference locations were tested statistically using ANOVAs and t-tests. Atmospheric fixation of CO_2 in the wetland was estimated from aquatic biomass C production (Supplementary Table 3). Uncertainties in aggregated C fluxes (Table 1) were propagated using variance-based error propagation, accounting explicitly for shared discharge terms and covariance among flux components,

To contextualise the resulting C budget of the beaver wetland, we developed a counterfactual stream corridor scenario without beavers (Supplementary Table 1; Supplementary Text 8) and further scaled potential C sequestration benefits at a national scale of Switzerland (Supplementary Text 9).

Reporting summary

Further information on research design is available in the Nature Portfolio Reporting Summary linked to this article.

Data availability

Hydrology, bathymetry, and carbon flux data, together with measured and projected sediment carbon content are openly available from the following repository: <https://doi.org/10.6084/m9.figshare.29500514>⁴¹.

Received: 1 July 2025; Accepted: 30 January 2026;

Published online: 18 March 2026

References

- Battin, T. J. et al. River ecosystem metabolism and carbon biogeochemistry in a changing world. *Nature* **613**, 449–459 (2023).
- Vidon, P. et al. Hot spots and hot moments in riparian zones: potential for improved water quality management. *JAWRA J. Am. Water Resour. Assoc.* **46**, 278–298 (2010).
- Hotchkiss, E. R. et al. Sources of and processes controlling CO_2 emissions change with the size of streams and rivers. *Nat. Geosci.* **8**, 696–699 (2015).
- Wollheim, W. M. et al. River network saturation concept: factors influencing the balance of biogeochemical supply and demand of river networks. *Biogeochemistry* **141**, 503–521 (2018).
- Lauerwald, R., Laruelle, G. G., Hartmann, J., Ciais, P. & Regnier, P. A. G. Spatial patterns in CO_2 evasion from the global river network. *Glob. Biogeochem. Cycles* **29**, 534–554 (2015).
- Dewey, C. et al. Beaver dams overshadow climate extremes in controlling riparian hydrology and water quality. *Nat. Commun.* **13**, 6509 (2022).
- Larsen, A., Larsen, J. R. & Lane, S. N. Dam builders and their works: Beaver influences on the structure and function of river corridor hydrology, geomorphology, biogeochemistry and ecosystems. *Earth-Sci. Rev.* **218**, 103623 (2021).
- Nummi, P., Vehkaoja, M., Pumpanen, J. & Ojala, A. Beavers affect carbon biogeochemistry: both short-term and long-term processes are involved. *Mammal. Rev.* **48**, 298–311 (2018).
- Wohl, E. Landscape-scale carbon storage associated with beaver dams. *Geophys. Res. Lett.* **40**, 3631–3636 (2013).
- Jarvie, H. P., King, S. M. & Neal, C. Inorganic carbon dominates total dissolved carbon concentrations and fluxes in British rivers: application of the *THINCARB* model – Thermodynamic modelling of inorganic carbon in freshwaters. *Sci. Total Environ.* **575**, 496–512 (2017).
- Chaubey, I. & Ward, G. M. Hydrologic budget analysis of a small natural wetland in Southeast USA. *J. Environ. Inform.* **8**, 10–21 (2006).
- Graham, H. A., Puttock, A. K., Elliott, M., Anderson, K. & Brazier, R. E. Exploring the dynamics of flow attenuation at a beaver dam sequence. *Hydrol. Process.* **36**, e14735 (2022).

13. Puttock, A., Graham, H. A., Cunliffe, A. M., Elliott, M. & Brazier, R. E. Eurasian beaver activity increases water storage, attenuates flow and mitigates diffuse pollution from intensively-managed grasslands. *Sci. Total Environ.* **576**, 430–443 (2017).
14. Boodoo, K. S., Schelker, J., Trauth, N., Battin, T. J. & Schmidt, C. Sources and variability of CO₂ in a prealpine stream gravel bar. *Hydrol. Process.* **33**, 2279–2299 (2019).
15. Russo, T. A., Fisher, A. T. & Roche, J. W. Improving riparian wetland conditions based on infiltration and drainage behavior during and after controlled flooding. *J. Hydrol.* **432–433**, 98–111 (2012).
16. Naiman, R. J., Melillo, J. M. & Hobbie, J. E. Ecosystem alteration of boreal forest streams by beaver (*Castor Canadensis*). *Ecology* **67**, 1254–1269 (1986).
17. IPCC. Climate Change 2023: Synthesis Report. Contribution of Working Groups I, II and III to the Sixth Assessment Report of the Intergovernmental Panel on Climate Change. *IPCC Geneva Switz.* 35–115 (IPCC, 2023).
18. Duvert, C., Butman, D. E., Marx, A., Ribolzi, O. & Hutley, L. B. CO₂ evasion along streams driven by groundwater inputs and geomorphic controls. *Nat. Geosci.* **11**, 813–818 (2018).
19. Klaus, M. Decadal increase in groundwater inorganic carbon concentrations across Sweden. *Commun. Earth Environ.* **4**, 221 (2023).
20. Craft, C., Vymazal, J. & Kröpfelová, L. Carbon sequestration and nutrient accumulation in floodplain and depressional wetlands. *Ecol. Eng.* **114**, 137–145 (2018).
21. FOEN. Switzerland’s Greenhouse Gas Inventory 1990–2021: National Inventory Document. Submission of April 2023 under the United Nations Framework Convention on Climate Change. *Fed. Off. Environ. Bern* <https://www.bafu.admin.ch/bafu/en/home/topics/climate/state/data/climate-reporting/ghg-inventories/latest.html> (BAFU, 2023).
22. Gibbs, D. A. et al. Revised and updated geospatial monitoring of 21st century forest carbon fluxes. *Earth Syst. Sci. Data* **17**, 1217–1243 (2025).
23. Min, S.-K., Zhang, X., Zwiers, F. W. & Hegerl, G. C. Human contribution to more-intense precipitation extremes. *Nature* **470**, 378–381 (2011).
24. Smufer, F., Casas-Ruiz, J. P., St-Pierre, A. & del Giorgio, P. A. Integrating beaver ponds into the carbon emission budget of boreal aquatic networks: a case study at the watershed scale. *Ecosystems* **26**, 1309–1325 (2023).
25. Weyhenmeyer, C. E. Methane emissions from beaver ponds: rates, patterns, and transport mechanisms. *Glob. Biogeochem. Cycles* **13**, 1079–1090 (1999).
26. Dennis, M., Angst, C., Larsen, J. R., Rey, E. & Larsen, A. A national scale floodplain model revealing channel gradient as a key determinant of beaver dam occurrence and inundation potential can anticipate land-use based opportunities and conflicts for river restoration. *Glob. Ecol. Conserv.* **56**, e03304 (2024).
27. Mayer, S. et al. Soil organic carbon sequestration in temperate agroforestry systems—a meta-analysis. *Agric. Ecosyst. Environ.* **323**, 107689 (2022).
28. Poeplau, C. & Don, A. Carbon sequestration in agricultural soils via cultivation of cover crops—a meta-analysis. *Agric. Ecosyst. Environ.* **200**, 33–41 (2015).
29. Serva, D., Biondi, M. & Iannella, M. The Eurasian beaver range expansion reveals uneven future trends and possible conservation issues: an European assessment. *Biodivers. Conserv.* **32**, 1999–2016 (2023).
30. Butler, D. R. & Malanson, G. P. The geomorphic influences of beaver dams and failures of beaver dams. *Geomorphology* **71**, 48–60 (2005).
31. Marston, R. River Entrenchment in small Mountain Valleys of the Western USA: influence of beaver, grazing and clearcut logging / L’incision des cours d’eau dans les petites vallées montagnardes de l’ouest américain: l’influence des castors, du pâturage et des coupes forestières à blanc. <https://doi.org/10.3406/geoca.1994.4232> (1994).
32. Persico, L. & Meyer, G. Holocene beaver damming, fluvial geomorphology, and climate in Yellowstone National Park, Wyoming. *Quat. Res.* **71**, 340–353 (2009).
33. Day, T. J. & Day, T. T. Field procedures and evaluation of a slug dilution gauging method in mountain streams. *J. Hydrol. N. Z.* **16**, 113–133 (1977).
34. McCleskey, R. B., Runkel, R. L., Murphy, S. F. & Roth, D. A. Stream discharge determinations using slug additions and specific conductance. *Water Resour. Res.* **61**, e2024WR037771 (2025).
35. Weijts, S. V., Mutzner, R. & Parlange, M. B. Could electrical conductivity replace water level in rating curves for alpine streams? *Water Resour. Res.* **49**, 343–351 (2013).
36. Priestley, C. H. B. & Taylor, R. J. On the assessment of surface heat flux and evaporation using large-scale parameters. https://journals.ametsoc.org/view/journals/mwre/100/2/1520-0493_1972_100_0081_otaosh_2_3_co_2.xml (1972).
37. Hirsch, R. M., Moyer, D. L. & Archfield, S. A. Weighted regressions on time, discharge, and season (WRTDS), with an application to Chesapeake Bay River Inputs. *JAWRA J. Am. Water Resour. Assoc.* **46**, 857–880 (2010).
38. Hirsch, R. M., Archfield, S. A. & De Cicco, L. A. A bootstrap method for estimating uncertainty of water quality trends. *Environ. Model. Softw.* **73**, 148–166 (2015).
39. Fuss, R. Greenhouse gas flux calculation from chamber measurements. R package version 0.7. <https://CRAN.R-project.org/package=gasfluxes> (CRAN, 2024).
40. Moritz, S. & Bartz-Beielstein, T. imputeTS: time series missing value imputation in. *R. R. J.* **9**, 207–218 (2017).
41. Hallberg, L. et al. Data from: beavers can convert stream corridors to persistent carbon sinks. [Dataset]. figshare. <https://doi.org/10.6084/m9.figshare.29500514> (2025).

Acknowledgements

We thank Kasper Berger for field assistance and we are grateful to Linus Fässler, Livia Vogel, Maarika Bischoff, Daniela Fischer, Denise Freudemann, and team for their support with laboratory analysis. We also thank Peter Leiser for chamber construction and technical support, and Thierry Adatte for Rock-Eval analysis. This work was supported by the UK Natural Environmental Research Council NE/V021117/1 (J.R.L., M.D.), the Swiss Federal Office for the Environment BAFU-417.12-06-.3-01-4/2 (C.A., A.L., J.R.L., B.S.), and by the Ramón y Cajal Fellowship RYC2022-038407-I (J.B.).

Author contributions

L.H.: conceptualisation, methodology, formal analysis, investigation, writing – original draft, review and editing, visualisation. J.R.L., A.L., N.C., B.S., and M.D.: conceptualisation, methodology, validation, formal analysis, resources, writing – review and editing, project administration, funding acquisition. R.E. and T.R.B.: data collection, formal analysis, investigation, writing – review and editing, visualisation. S.T.: methodology, data collection, investigation, writing – review and editing. J.B.: methodology, validation, writing – review and editing. C.A.: conceptualisation, funding acquisition, writing – review and editing.

Competing interests

The authors declare no competing interests.

Additional information

Supplementary information The online version contains supplementary material available at <https://doi.org/10.1038/s43247-026-03283-8>.

Correspondence and requests for materials should be addressed to Lukas Hallberg.

Peer review information *Communications Earth and Environment* thanks the anonymous reviewers for their contribution to the peer review of this work. Primary Handling Editors: Somaparna Ghosh [A peer review file is available].

Reprints and permissions information is available at <http://www.nature.com/reprints>

Publisher's note Springer Nature remains neutral with regard to jurisdictional claims in published maps and institutional affiliations.

Open Access This article is licensed under a Creative Commons Attribution 4.0 International License, which permits use, sharing, adaptation, distribution and reproduction in any medium or format, as long as you give appropriate credit to the original author(s) and the source, provide a link to the Creative Commons licence, and indicate if changes were made. The images or other third party material in this article are included in the article's Creative Commons licence, unless indicated otherwise in a credit line to the material. If material is not included in the article's Creative Commons licence and your intended use is not permitted by statutory regulation or exceeds the permitted use, you will need to obtain permission directly from the copyright holder. To view a copy of this licence, visit <http://creativecommons.org/licenses/by/4.0/>.

© The Author(s) 2026